phys. stat. sol. (b) **243**, No. 7, 1706–1712 (2006) / **DOI** 10.1002/pssb.200565378

Quantum transport in high mobility AlGaN/GaN 2DEGs and nanostructures

S. Schmult[*, 1], **M. J. Manfra**[1], **A. M. Sergent**[1], **A. Punnoose**[1], **H. T. Chou**[2], **D. Goldhaber-Gordon**[3], and **R. J. Molnar**[4]

[1] Bell Laboratories, Lucent Technologies, 600 Mountain Ave, Murray Hill, NJ 07974, USA
[2] Department of Applied Physics, Stanford University, Stanford, CA 94305, USA
[3] Department of Physics, Stanford University, Stanford, CA 94305, USA
[4] MIT Lincoln Laboratory, 244 Wood Street, Lexington, MA 02420, USA

Received 15 August 2005, revised 9 January 2006, accepted 18 January 2006
Published online 9 June 2006

PACS 73.21.–b, 73.40.Kp, 73.63.–b

High mobility two-dimensional electron systems in GaN/AlGaN heterostructures have been realized by plasma assisted molecular beam epitaxy on GaN templates. In the density range of 10^{11} cm^{-2} to 10^{12} cm^{-2}, mobility values exceeding 160 000 cm^2/Vs have been achieved. Scattering mechanisms that presently limit the production of higher mobility samples are discussed. We present results of a systematic study of the weak localization and antilocalization corrections to the classical conductivity at very low magnetic fields. The unambiguous observation of a conductivity maximum at $B = 0$ suggests that spin–orbit scattering is not negligible in GaN heterostructures as one might expect for a wide-bandgap system. We have recently realized electron transport through GaN nanostructures. We report on the transport properties of the first quantum point contacts (QPCs) in GaN. These devices are used to study one-dimensional transport in the Nitride system.

1 Introduction

Many experiments on mesoscopic semiconductor systems have been based on GaAs/AlGaAs heterostructures. Reasons include clean interfaces accompanied with an almost perfect lattice match, and mature growth and processing techniques developed over the last 30 years. GaN with a much larger band gap compared to GaAs, has drawn recent interest in industry for the use in blue laser diodes and microwave power field-effect transistors. GaN/AlGaN heterostructures also possess some unique physical properties that are of fundamental interest. First, no modulation doping is needed to produce a two-dimensional electron gas: the reduced symmetry of the crystal structure induces a spontaneous polarization and the lattice mismatch between GaN and AlGaN induces a piezoelectric polarisation, the combination of both causes a two-dimensional electron gas accumulated at the interface [1]. Avoiding doping removes one major source of scattering. Second, the higher effective electron mass of $\sim 0.2 m_e$ (0.067 in GaAs) [2, 3] and the lower dielectric constant of ~9 (~13 in GaAs) make electron–electron interactions in GaN more important. Third, the g-factor of ~2 (–0.44 in GaAs) makes it easier to manipulate electron spins with magnetic fields. In order to utilize the unique material properties of GaN for physics experiments, a high mobility two-dimensional electron gas (2DEG) is required.

[*] Corresponding author: e-mail: schmult@lucent.com, Phone: +1 908 582 7263, Fax: +1 908 582 4868

During the last few years, ongoing efforts to improve the mobility of two-dimensional electron gases in the GaN/AlGaN material system have made rapid progress. Two groups have recently and independently reported mobility over 100 000 cm^2/Vs [4, 5]. A key ingredient to higher mobility is the ever-improving quality of GaN templates used in molecular beam epitaxy (MBE) growth. It has now been established that in the density range $<10^{12}$ cm^{-2} the electron mobility is limited by long-range Coulomb scattering from charged threading dislocations with densities $>10^8$ cm^{-2} [6, 7]. In order to improve mobility we must therefore work with GaN templates with dislocation densities significantly below 10^8 cm^{-2}. Improvements in the quality of our GaN templates grown by hydride vapour phase epitaxy (HVPE) have directly resulted in record low-temperature mobility.

2 Growth and characterization of high electron mobility AlGaN/GaN 2DEGs

The heterostructures discussed here were grown by plasma-assisted molecular beam epitaxy on 50 mm GaN templates prepared by HVPE. The HVPE templates are typically 100 μm thick and are known to have threading dislocation densities of $<10^8$ cm^{-2}. The HVPE GaN has been compensated with Zinc at a level of $\sim 10^{17}$ cm^{-2} to suppress any residual conductivity that may obscure the observation of the 2DEG properties at very low carrier densities. In these structures no parasitic conduction is observed from room temperature down to 300 mK, even at electron densities of $\sim 3 \times 10^{11}$ cm^{-2}. The MBE grown epitaxial layer sequence consists of a 1 μm thick GaN buffer followed by a 16 nm $Al_xGa_{1-x}N$ undoped barrier capped with ~2 nm GaN. The Al mole fraction x varies between 0.05 and 0.1 to cover a wide range in electron density and has been verified in reference samples by X-ray diffraction. The entire structure is grown under slightly Ga-rich conditions at a substrate temperature of ~745 °C with the nitrogen plasma source power set to 205 W and a nitrogen flow rate of 0.50 sccm. The MBE operating pressure during growth is $\sim 2 \times 10^{-6}$ Torr maintained by two closed-cycle ^{4}Helium cryopumps.

Upon completion of growth, the samples are processed into Hall bars for electrical characterization. The Hall bar is 100 μm wide by 2 mm long. Fourteen voltage probes are placed symmetrically along the

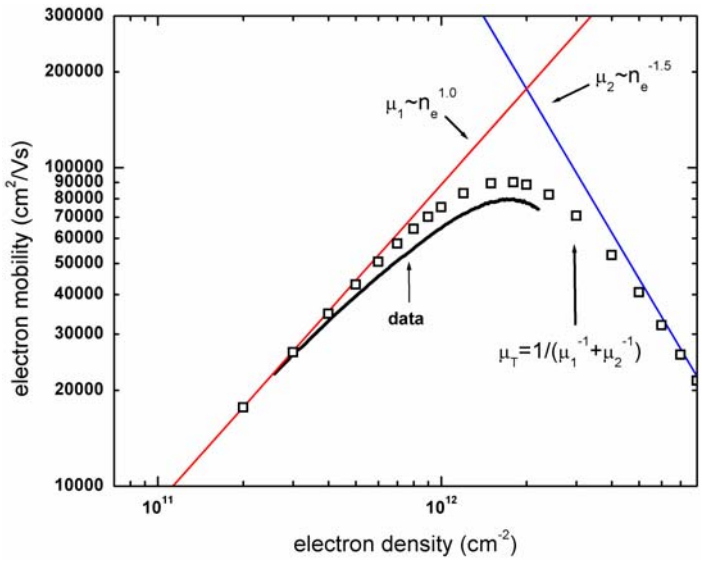

Fig. 1 (online colour at: www.pss-b.com) Electron mobility versus density in a gated Hall bar at 300 mK. The solid black curve is the experimentally measured mobility. For comparison, the red line displays the function $\mu_1 \sim n_e^1$ at low density and the blue line represents $\mu_2 \sim n_e^{-1.5}$ in the high-density regime. The open black squares are calculated from $\mu_T = 1/(\mu_1^{-1} + \mu_2^{-1})$.

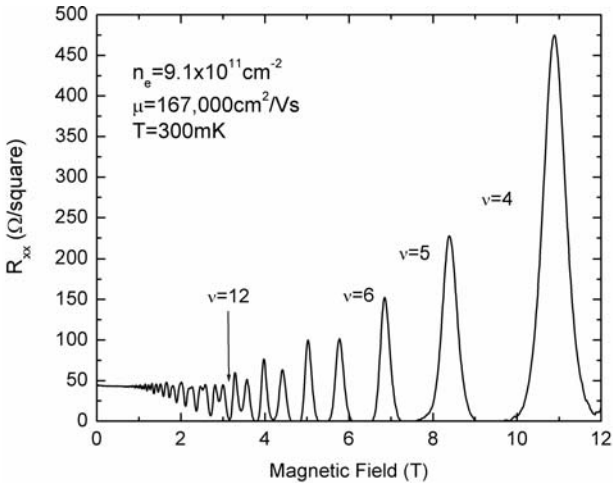

Fig. 2 Longitudinal resistance of a high mobility 2DEG grown on HVPE GaN. The Shubnikov–de-Haas oscillations commence at 0.6 T.

device. Mesas of 100 nm height are defined with a chlorine-based dry etch. Ohmic contacts consist of a Ti/Al/Ni/Au metal stack that is thermally annealed at 750 °C for 30 sec. These simple Hall bar structures are used for preliminary characterization of the wafer's sheet carrier density and mobility. In order to control the density within a single device, insulated gate field-effect transistors (FETs) are also used. After Ohmic contact definition, 50 nm of SiO_2 is deposited on the Hall bar. The additional SiO_2 layer results in suppressed gate leakage current. Finally 10 nm of Ni and 100 nm of Au are deposited over the SiO_2 along the Hall bar forming an insulated gate structure. At $T = 0.3$ K, the gate leakage is insignificant (<1 nA) over a wide range of gate voltages.

3 Transport properties of 2DEGs

Measurement of the longitudinal (R_{xx}) and transverse (R_{xy}) magnetoresistance is carried out in ^{3}He cryostat operated at a base temperature of 300 mK. A measuring current of ≤1 μA at a frequency of 13 Hz is used. R_{xx} and R_{xy} are detected using standard lock-in techniques. Figure 1 displays mobility vs. density for a typical FET. For low densities up to 1×10^{12} cm^{-2} the mobility rapidly increases with increasing density. In this sample the mobility peaks at 80 000 cm^2/Vs, and then decreases for further increase of density. This decrease above 2×10^{12} cm^{-2} is known to be a consequence of increased alloy and interface roughness scattering [8–10]. In the low-density regime, the mobility is limited by Coulomb scattering mainly from charged surface states, background impurities and charged dislocations [11, 12]. The actual peak mobility value and sheet density at which the peak occurs depends on the relative strength of these competing mechanisms. The solid black curve in Fig. 1 is the experimentally measured mobility. For comparison, the red line displays the function $\mu_1 \sim n_e^1$ at low density and the blue line represents $\mu_2 \sim n_e^{-1.5}$ in the high-density regime. The open black squares are calculated from $\mu_T = 1/(\mu_1^{-1} + \mu_2^{-1})$.

The magnetic field dependent longitudinal resistance for a high mobility 2DEG [4] is shown in Fig. 2. This sample exhibits low temperature mobility of 167 000 cm^2/Vs at a density of 9.1×10^{11} cm^{-2}. The integral Quantum Hall Effect is fully developed at a magnetic field of 3 T and the onset of the Shubnikov–de-Haas (SdH) oscillations is visible below 1 T at a temperature of 300 mK.

4 Spin–orbit coupling in GaN

At present, the role of spin–orbit coupling in GaN heterostructures is not well understood. In order to study spin–orbit coupling in our GaN/AlGaN heterostructures, we have systematically studied the weak localization and antilocalization corrections to the classical conductivity at very low magnetic fields. It is well established that a maximum in longitudinal conductivity at $B = 0$ originates from spin–orbit cou-

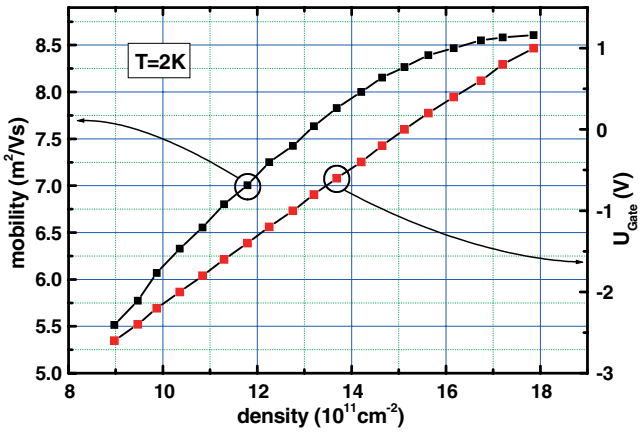

Fig. 3 (online colour at: www.pss-b.com) Electron mobility versus density in a gated 2DEG used for the study of spin–orbit coupling.

pling [13, 14]. The unambiguous observation of a conductivity maximum at $B = 0$ in our data suggests that spin–orbit coupling is not negligible in GaN heterostructures as one might expect for a wide band-gap material system. In a gate tunable sample we examined the density dependent behavior of the antilocalization feature. Figure 3 shows the mobility versus density and gate voltage for the investigated sample. Here it is possible to tune the density from 9×10^{11} cm^{-2} to 1.8×10^{12} cm^{-2}, resulting in mobilities between 55 000 cm^2/Vs and 86 000 cm^2/Vs.

In Fig. 4 magneto-conductance data are shown for different densities at a temperature of 300 mK. The data are plotted as the change in conductivity, $\Delta\sigma = \sigma_{square}(B) - \sigma_{square}(B = 0)$, with $\sigma_{square}(B) = 1/R_{square}(B)$ and $\sigma_{square}(B = 0) = 1/R_{square}(B = 0)$. This data reveals a conductivity maximum at $B = 0$ and a conductivity minimum at $B \sim 2$ mT which is symmetric in magnetic field. The magnetic field position of the minima is determined by the strength of the spin–orbit coupling. Here we note that the field position of the conductivity minima does not change over this fairly narrow density range. This suggests that the strength of spin–orbit coupling (the spin-relaxation rate) is not changing dramatically. However, the amplitude of the central conductivity peak does change significantly over this density range. The amplitude of the peak is governed by the ratio of the phase-breaking and spin-relaxation rates. For smaller phase-breaking rate and larger spin-relaxation the amplitude of the antilocalization peak is enhanced. As we move to lower density and mobility, the phase-breaking rate becomes larger such that the antilocalization feature is diminished.

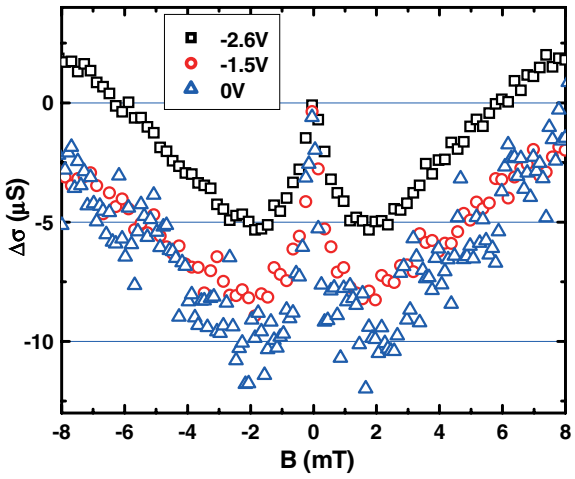

Fig. 4 (online colour at: www.pss-b.com) Magneto-conductivity data at a temperature of 300 mK for different gate voltages (for corresponding densities see Fig. 3). The magnetic field position of the minima does not change within the measurement accuracy, while the amplitude of the antilocalization feature is largest for the highest density and mobility.

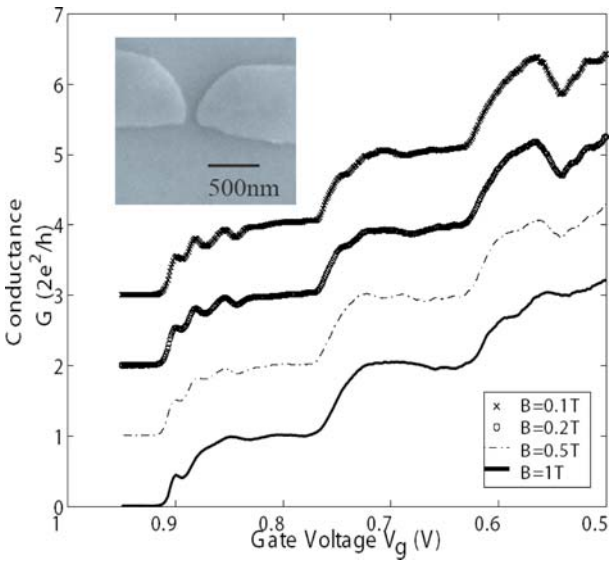

Fig. 5 (online colour at: www.pss-b.com) GaN QPC was measured at 300 mK. It shows well-quantized plateaus with resonances. The resonances were reduced after increasing the magnetic field to 1 T. 1 T is considered as low field in our experiment because of the high 2DEG density in our GaN heterostructure. The inset shows the split-gate GaN QPC we fabricated, the width of the constriction between the two gates is 80 nm.

5 One-dimensional transport: quantum point contacts

A quantum point contact (QPC) is a narrow constriction between two electron reservoirs. The width of the constriction can be tuned to pass one or more channels of electrons, each with a quantized conductance of $2e^2/h$. The devices investigated in this work are fabricated on a GaN/AlGaN heterostructure with a 2DEG formed 19 nm below the surface. The 2DEG has a low temperature mobility of 56 000 cm^2/Vs at a density of 1.0×10^{12} cm^{-2}. Ti/Al metal pads were annealed to contact the 2DEG. Next, a mesa was patterned by photolithography followed by a Cl-based plasma etch. The split-gate structure that forms the QPC was realized by electron beam lithography followed by evaporation and liftoff of Ni gates (Fig. 5, inset). The low temperature differential conductance $G = dI/dV_{sd}$ was measured at 300 mK using a lock-in technique with a 20 μV, 77 Hz excitation added to a variable dc voltage V_{sd} applied between source and drain.

Near zero magnetic field the linear conductance $G = dI/dV_{sd}$ ($V_{sd} = 0$) shows two clear quantized plateaus at $2e^2/h$ and $4e^2/h$ (Fig. 5). The third and fourth plateaus are obscured by resonances that might be

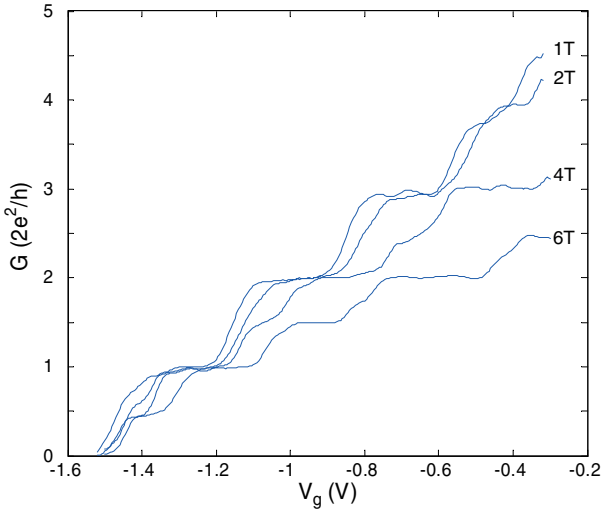

Fig. 6 Linear conductance $G(V_g)$ at perpendicular magnetic field B = 1 T, 2 T, 4 T and 6 T. Spin-split plateaus at multiples of e^2/h start to appear at 4 T.

caused by backscattering from defects: the mean free path in the system is only 700 nm, comparable to the largest features of the split-gate structure. A small perpendicular magnetic field improves the quantization of the plateaus. Several resonances periodic in gate voltage are evident at $B = 0.1$ T. As the magnetic field is increased to 1 T, the third plateau appears clearly and the resonances are suppressed as backscattering is reduced by the perpendicular magnetic field.

A strong magnetic field induces a large Zeeman energy difference ($g^*\mu_B B$) between spin up and spin down subbands. This energy difference results in conductance quantized in units of e^2/h rather than $2e^2/h$. Figure 6 shows the linear conductance $G(V_g)$ at four different perpendicular magnetic fields. In addition to its effect on spin in a QPC a perpendicular magnetic field changes subband energies by adding an extra effective lateral confinement. This does not alter the 1D nature of transport in our QPC and does not further discriminate between different spin states. Each quantum plateau simply becomes longer in higher magnetic fields because of the larger subband energy. At $B = 1$ T, three conductance plateaus quantized in units of $2e^2/h$ are observed and a shoulder emerges below the first plateau. At $B = 4$ T spin-split plateaus e^2/h, $3e^2/h$, $5e^2/h$ have already formed and they are more pronounced at 6 T. From these measurements an effective Landé g-factor of 2.5 is derived [15].

6 Summary and conclusion

High mobility two-dimensional electron systems in GaN/AlGaN heterostructures have been grown by MBE on HVPE GaN templates with electron densities $<10^{12}$ cm^{-2}. A maximum electron mobility of 167 000 cm^2/Vs was achieved. In these samples the integer Quantum Hall Effect is fully developed at magnetic fields around 3 T, with Shubnikov–de-Haas oscillations commencing below 1 T. In GaN/AlGaN heterostructures antilocalization at low magnetic fields has been observed. The appearance of this antilocalization feature suggests that spin–orbit coupling is strong in GaN. The origin of the strong coupling is still under investigation. In addition, high electron mobility two-dimensional GaN systems have been used to demonstrate ballistic transport in one-dimensional Quantum Point Contacts.

Acknowledgements DGG acknowledges the Office of Naval Research Young Investigator Program, Award No. N00014-01-1-0569 and Stanford's Center of Integrated Systems. The Lincoln Laboratory portion of this work was sponsored by the United States Air Force under Air Force contract number FA8721-05-C-0002. The opinions, interpretations, conclusions and recommendations are those of the authors and are not necessarily endorsed by the United States Government.

References

[1] O. Ambacher, J. Smart, J. R. Shealy, N. G. Weimann, K. Chu, M. Murphy, W. J. Schaff, L. F. Eastman, R. Dimitrov, L. Wittmer, M. Stutzmann, W. Rieger, and J. Hilsenbeck, J. Appl. Phys. **85**, 3222 (1999).
[2] S. Syed, J. B. Heroux, Y. J. Wang, M. J. Manfra, R. J. Molnar, and H. L. Stormer, Appl. Phys. Lett. **83**, 4553 (2003).
[3] W. Knap, E. Frayssinet, M. L. Sadowski, C. Skierbiszewski, D. Maude, V. Falko, M. Asif Khan, and M. S. Shur, Appl. Phys. Lett. **75**, 3156 (1999).
[4] M. J. Manfra, K. W. Baldwin, A. M. Sergent, K. W. West, R. J. Molnar, and J. Cassie, Appl. Phys. Lett. **85**, 5394 (2004).
[5] C. Skierbiszewski, K. Dybko, W. Knap, M. Siekacz, W. Krupczynski, G. Nowak, M. Bockowski, J. Lusakowski, Z. R. Wasilewski, D. Maude, T. Suski, and S. Porowsi, Appl. Phys. Lett. **86**, 102106 (2005).
[6] M. J. Manfra, K. W. Baldwin, A. M. Sergent, R. J. Molnar, and J. Cassie, Appl. Phys. Lett. **85**, 1722 (2004).
[7] M. J. Manfra, S. Simon, K. W. Baldwin, A. M. Sergent, R. J. Molnar, and J. Cassie, Appl. Phys. Lett. **85**, 5278 (2004).
[8] M. J. Manfra, L. N. Pfeiffer, K. W. West, H. L. Stormer, K. W. Baldwin, J. W. P. Hsu, D. V. Lang, and R. J. Molnar, Appl. Phys. Lett. **77**, 2888 (2000).
[9] I. P. Smorchkova, C. R. Elsass, J. P. Ibbetson, R. Ventry, B. Heying, P. Fini, E. Haus, S. P. DenBaars, J. S. Speck, and U. K. Mishra, J. Appl. Phys. **86**, 4520 (1999).
[10] L. Hsu and W. Walukiewicz, J. Appl. Phys. **89**, 1783 (2001).

[11] L. Hsu and W. Walukiewicz, Appl. Phys. Lett. **80**, 2508 (2002).
[12] D. Jena, I. Smorchkova, A. C. Gossard, and U. K. Mishra, phys. stat. sol. (b) **228**, 617 (2001).
[13] W. Knap, C. Skierbiszewski, A. Zduniak, E. Litwin-Staszewska, D. Bertho, F. Kobbi, J. L. Robert, G. E. Pikus, F. G. Pikus, S. V. Iordanskii, V. Mosser, K. Zekentes, and Yu. B. Lyanda-Geller, Phys. Rev. B **53**, 3912 (1996).
[14] J. B. Miller, D. M. Zumbühl, C. M. Marcus, Y. B. Lyanda-Geller, D. Goldhaber-Gordon, K. Campman, and A. C. Gossard, Phys. Rev. Lett. **90**, 076807 (2003).
[15] H. T. Chou, S. Lüscher, D. Goldhaber-Gordon, M. J. Manfra, A. M. Sergent, K. W. West, and R. J. Molnar, Appl. Phys. Lett. **86**, 073108 (2005).

